

Author's Accepted Manuscript

Transports and pathways of overflow water in the Rockall Trough

Clare Johnson, Toby Sherwin, Stuart Cunningham, Estelle Dumont, Loïc Houpert, N. Penny Holliday



PII: S0967-0637(16)30250-3
DOI: <http://dx.doi.org/10.1016/j.dsr.2017.02.004>
Reference: DSR12755

To appear in: *Deep-Sea Research Part I*

Received date: 5 August 2016
Revised date: 8 February 2017
Accepted date: 10 February 2017

Cite this article as: Clare Johnson, Toby Sherwin, Stuart Cunningham, Estelle Dumont, Loïc Houpert and N. Penny Holliday, Transports and pathways of overflow water in the Rockall Trough, *Deep-Sea Research Part I* <http://dx.doi.org/10.1016/j.dsr.2017.02.004>

This is a PDF file of an unedited manuscript that has been accepted for publication. As a service to our customers we are providing this early version of the manuscript. The manuscript will undergo copyediting, typesetting, and review of the resulting galley proof before it is published in its final citable form. Please note that during the production process errors may be discovered which could affect the content, and all legal disclaimers that apply to the journal pertain.

Transports and pathways of overflow water in the Rockall Trough

Authors: Clare Johnson^{1*}, Toby Sherwin¹, Stuart Cunningham¹, Estelle Dumont¹, Loïc Houpert¹, N. Penny Holliday²

¹ *Scottish Association for Marine Science, Oban, UK.*

² *National Oceanography Centre, Southampton, UK.*

* corresponding author

clare.johnson@sams.ac.uk

SAMS, Scottish Marine Institute, Oban, Argyll, PA37 1QA, Scotland.

Accepted manuscript

Abstract

Water mass analysis reveals a persistent core of deep overflow water within the Rockall Trough which hugs the northern and western boundaries of the basin. Mean speeds within this overflow are 10-15 cm s⁻¹ giving a transport time from the Wyville Thomson Ridge to the central basin of < 50 days. Analysis of the 40-year Extended Ellett Line record shows proportions of Norwegian Sea Deep Water associated with the deep core exceed 15 % around one quarter of the time. We present the first transport estimates for overflow water in the Rockall Trough. This flux is for overflow water modified by mixing with a density greater than 27.65 kg m⁻³. Mean values calculated both from a newly deployed mooring array (OSNAP project) and indirectly from the Extended Ellett Line time-series are -0.3 ± 0.04 Sv. Although the flux is highly variable there is no long term trend. As some overflow appears to exit into the Iceland Basin via channels between the northern banks, we suggest that the volume transport will likely increase as the flow pathway is traced back around the boundary of the Rockall Trough towards the Wyville Thomson Ridge.

Key words

Rockall Trough; Extended Ellett Line; OSNAP; Wyville Thomson Ridge Overflow Water

Highlights

- flow pathway deep overflow around northern and western boundary
- transport time Wyville Thomson Ridge to central trough < 50 days
- > 15 % Norwegian Sea Deep Water seen one quarter of time
- transport modified WTOW (> 27.65 kg m⁻³) at 57.5 °N -0.3 ± 0.04 Sv
- no trend in transport over past 40 years

1. Introduction

Flow in the eastern subpolar North Atlantic is an important component of the global thermohaline circulation. Around 50 % of the upper ocean inflow to the Nordic Seas passes through the Rockall Trough and over the Wyville Thomson Ridge, and just under 50 % of the cold dense outflow returns through the Faroese Channels (Hansen and Østerhus, 2000). Although most of the return flow exits through the Faroe Bank Channel into the Iceland Basin (2.2 Sv; Hansen *et al.*, 2016), around 10-15 % spills over the Wyville Thomson Ridge into the Rockall Trough (Dickson and Brown, 1994; Hansen and Østerhus, 2000). Thirty months of sustained current meter measurements estimate the mean transport of Wyville Thomson Ridge Overflow Water (WTOW) as > 0.2 Sv for water colder than 0°C , and ~ 0.9 Sv when entrained Atlantic Waters are included (Sherwin *et al.*, 2008). Whilst the WTOW flux forms only 5 % of the total return flow across the Greenland-Scotland Ridge (Dickson and Brown, 1994; Hansen and Østerhus, 2000), it is comparable to that of other overflow waters which have been identified at considerable distances from their source; for example that exiting the Mediterranean Sea (0.68 Sv, Bryden *et al.*, 1994) and Red Sea (0.35 Sv, Murray and Johns, 1997).

Although overflow water has been known to enter the Rockall Trough for several decades (e.g. Ellett and Roberts, 1973; Sherwin and Turrell, 2005), the signature of the water mass has only been established recently. In a qualitative analysis, Johnson *et al.* (2010) showed that WTOW exists both as a wide-spread intermediate water mass and a denser deeper component which is confined to the western portion of the basin. Intermediate WTOW was observed in around 75 % of the long-running Extended Ellett Line (EEL) record at 57.5°N in the Rockall Trough, whilst the deeper component was observed approximately 40 % of the time. Prior to this study, several observations of overflow water had been made in the northern and central trough (e.g. Ellett *et al.*, 1983; Harvey and Theodorou, 1986; New and Smythe-Wright, 2001), but there was uncertainty over the water masses identification, persistence and origins (e.g. Holliday *et al.*, 2000; Lee and Ellett, 1965). Whilst Johnson *et al.* (2010) established that WTOW is an important water mass within the Rockall Trough, the work primarily focussed on the less dense component of the overflow found in the intermediate water column. As such, questions remain on the pathways and transport of the denser deeper component of the overflow. Moorings were recently deployed in the central Rockall Trough as part of the North Atlantic wide Overturning in the Subpolar North Atlantic

Programme (OSNAP; Lozier *et al.*, in press) enabling direct transport estimates of WTOW to be determined within the basin for the first time.

In this paper we focus on the dense component of WTOW here termed deep WTOW. We first highlight the distribution of overflow water within the Rockall Trough by using water mass analysis to deconstruct the water column into its constituent water types. We then calculate the transport of WTOW with a density $>27.65 \text{ kg m}^{-3}$ using data from the first year of OSNAP measurements. We place this flux in context by computing geostrophic transports over the 40 year hydrographic record from the EEL. Finally, the results are discussed in conjunction with historical current meter records and previously published geological studies to derive a best estimate of pathways of dense overflow water in the Rockall Trough.

2. Background - signature of WTOW

As identification of WTOW in potential temperature – salinity (θ - S) space is vital to the water mass analysis discussed later; we briefly review previous work on the subject here. WTOW is formed as cold dense water flowing southward through the Faroese Channels overflows the Wyville Thomson Ridge (W, Figure 1) at the northern bound of the Rockall Trough (Ellett and Roberts, 1973; Sherwin and Turrell, 2005). Two deep water masses north of the ridge are potential sources for WTOW: Norwegian Sea Arctic Intermediate Water (NSAIW) and Norwegian Sea Deep Water (NSDW) (Turrell *et al.*, 1999). As these two water masses have a similar θ - S signature, previous studies have not been able to distinguish their relative contribution to WTOW (Hansen and Østerhus, 2000; Johnson *et al.*, 2010). However, the chlorofluorocarbon (CFC-11 and CFC-12) concentrations in the two water bodies are very different with higher values observed in NSAIW (Fogelqvist *et al.*, 2003). Hence, by using CFC data it is possible to determine that NSDW, rather than NSAIW, is the source for WTOW (Johnson, 2012). This finding is corroborated by the fact that the volume of NSAIW in contact with the Wyville Thomson Ridge is small due to north-south pinching of the layer (Cuthbertson *et al.*, 2014; Mauritzen *et al.*, 2005; Stashchuk *et al.*, 2011). Additionally, the isopycnal corresponding to NSDW uplifts in the vicinity of the Wyville Thomson Ridge to a depth above the ridge crest (Mauritzen *et al.*, 2005; Stashchuk *et al.*, 2011). As it overflows, NSDW mixes with the overlying northward-flowing upper waters (UW); hence, in θ - S space, water properties at the Wyville Thomson Ridge lie along a mixing line between the UW and

NSDW (light blue, Figure 2). This feature, which we refer to as the WTOW mixing line, is key to identifying overflow water in the Rockall Trough (Ellett *et al.*, 1983; Johnson *et al.*, 2010) and looks very different to the θ - S profile from the south-eastern entrance to the basin (green, Figure 2; Johnson *et al.*, 2010; Ullgren and White, 2010).

As mentioned, overflow water in the Rockall Trough is found both as an intermediate and deep water mass (Ellett *et al.*, 1983; Johnson *et al.*, 2010). We illustrate the signature of these two components by using example profiles from the 2006 EEL occupation (red / blue, Figure 2) when the influences of both intermediate and deep WTOW were particularly clear.

Intermediate WTOW is observed as a wide-spread layer lying below the UW and above the Mediterranean Overflow Water – Labrador Sea Water mixture (MOW-LSW). In θ - S space, water properties within this intermediate overflow (red / blue, 27.3-27.65 kg m⁻³, Figure 2) follow a similar trend to the WTOW mixing line observed at the Wyville Thomson Ridge (Johnson *et al.*, 2010). The bottom of the layer of intermediate overflow is identified by an inflexion point in θ - S space at around 27.65 kg m⁻³ (ISI, Figure 2). Here, water properties in the eastern part of the trough (red, Figure 2) move away from the WTOW mixing line to the MOW-LSW mixture which enters the Rockall Trough from the south. However, in the western half of the basin, a deep constituent of WTOW is also sometimes observed (blue, Figure 2; Johnson *et al.*, 2010). This denser component of the overflow water (> 27.65 kg m⁻³) can be identified as water below the mid-depth θ - S inflexion point whose properties are intermediate to the MOW-LSW and WTOW mixing lines (Johnson *et al.*, 2010). Hence, water that shows the presence of deep WTOW is more saline than water at the same density in the eastern portion of the basin (Johnson *et al.*, 2010; New and Smythe-Wright, 2001) and is easily identified using this criteria. For example, in 2006, the salinity at 27.8 kg m⁻³ on the eastern flank of Rockall Bank (blue, Figure 2) was 0.08 higher than at the same density in the east of the basin (red, Figure 2). Despite estimates suggesting that deep WTOW is only seen around 40 % of the time (Johnson *et al.*, 2010), the 1975-2015 mean salinity at 27.8 kg m⁻³ in the far west of the basin was still 0.04 higher than the mean salinity at the same density in the eastern trough.

3. Data

3.1. CTD data

Three sources of CTD (conductivity-temperature-depth) data are used within this work, all of which were obtained from the British Oceanographic Data Centre (www.bodc.ac.uk). The first is a one-off section across the northern Rockall Trough (BRS, Figure 1) which was occupied in May 2004 on board FRV Scotia (Sc0804). This CTD line runs north-south from Bill Baileys Bank to Rosemary Bank, and then south-eastwards to the Scottish Shelf. The second is another single-occupation section between two of the banks (Lousy Bank and George Bligh Bank) that separate the northern Rockall Trough from the Iceland Basin (LG, Figure 1). This line was occupied in October 1996 by RRS Discovery (D223). The final dataset is the EEL time-series (<http://projects.noc.ac.uk/ExtendedEllettLine>) which is a standard hydrographic section between Rockall and the Scottish Shelf along approximately 57.5 °N (EEL, Figure 1). This section began in 1975 and is currently jointly maintained by the Scottish Association for Marine Science and the National Oceanography Centre. In the 1970s and 1980s several occupations were made each year; however, since 1996 (when the section was extended to include the Iceland Basin) measurements have typically been made only once per year, usually between May and October (Holliday and Cunningham, 2013). Multiple instruments with varying precisions have been used over the 40 years, data were therefore rigorously quality checked. Any cruises with documented quality problems were discounted from this work; in particular noisy salinity data affected a number of cruises between 1979 and 1984. In total 50 sections with good quality data between 1975 and 2015 were analysed.

3.2. Mooring data

As part of the OSNAP programme, four moorings were deployed close to the Rockall Trough portion of the EEL for the first time in 2014 (blue triangles, Figure 1). This basin-wide array consists of three deep moorings (WB1, WB2 and EB1), and one Acoustic Doppler Current Profiler (ADCP) only mooring within a trawl resistant frame (ADCP1). All moorings were deployed in July 2014, except ADCP1 which was deployed in October 2014. The deep moorings consist of a number of Sea-Bird SBE37 microCAT CTDs and Nortek Aquadopp current profilers at various depths (Figure 3). All moorings were recovered in June 2015 and

subsequently re-deployed. Data were processed using the methods developed for the RAPID array (Rayner *et al.*, 2011); namely current data were corrected for magnetic deviations and speed of sound, before all data were filtered using a 40 hour Butterworth filter to remove any signals from tides and inertial oscillations. Data were then interpolated onto 12 hourly time-steps. In addition to the OSNAP data, records from three historical moorings on the northern and western boundaries of the Rockall Trough were also analysed (blue circles, Figure 1). These moorings were deployed in July 1978 as part of the Joint Air-Sea Interaction Experiment (JASIN). Data were obtained from BODC and were again low-pass filtered using the same 40 hour filter before being interpolated onto 12 hourly time-steps. Record lengths vary from 43 to 256 days (Table 1).

4. Methods

4.1. Water mass analysis

4.1.1. Details of water mass mixing model

A water mass mixing model was created so that the proportions of WTOW and its constituent water mass NSDW within the Rockall Trough could be quantified. Although we considered Optimum Multi-Parameter (OMP) analysis, the decision was made to use only potential temperature and salinity as model inputs. Perhaps the greatest strength of OMP is that it over-determines the mixing between water masses (e.g. Mackas *et al.*, 1987; Tomczak, 1981a); however, to achieve this additional input variables are required. High quality CFC data only exists for limited stations from a single EEL cruise (1997, D230) and not at all for the other two sections considered. Nutrient and oxygen data have been collected along the EEL since 1996, but some quality issues exist (Humphreys *et al.*, 2016; Johnson *et al.*, 2013). It is also worth noting that nutrients and oxygen are not conservative parameters meaning their distributions are affected by biogeochemical processes in addition to advection and mixing. The disadvantage to using only potential temperature and salinity is that assumptions must be made regarding the ability of water masses at different density levels to mix with one another. However, several studies employ this approach successfully (e.g. Castro *et al.*, 1998; Perez *et al.*, 2001; Rhein *et al.*, 2005). By using potential temperature and salinity data only, we were able to carry out mixing analysis over the entire 40 years of the EEL record. Additionally, we could look at the entire water column instead of having a vertical resolution limited by

discrete bottle samples. This is particularly advantageous when looking at a water mass such as deep WTOW which can be a relatively thin layer (Johnson *et al.*, 2010).

The six water types that influence the Rockall Trough were defined as points in θ - S space (Figure 4.a; Table 2) with mixing lines drawn from these. The designations for Antarctic Bottom Water (*AABW*), *MOW* and *NSDW* were fixed; however, the definitions for the lower bound of the UW ($UW_{(l)}$) and the upper and lower limits of LSW ($LSW_{(u)}$, $LSW_{(l)}$) were determined for each cruise. This accounts for the large temporal changes in these water masses related to the strength and extent of the subpolar gyre (e.g. Holliday, 2003; Lozier and Stewart, 2008). The mixing model assumed mixing between water lying on mixing lines rather than between individual water types. This is termed a percentage nomogram approach (Figure 4.b; Mamayev, 1975) and has been used in previous studies (e.g. Kirchner *et al.*, 2008; Rhein *et al.*, 2005; Tomczak, 1981b). In the eastern trough, water with a density between that of water types $UW_{(l)}$ and $LSW_{(u)}$ was considered to have formed from mixing between water lying on mixing lines $UW_{(l)}$ - B -(*NSDW*) and (*MOW*-) B - $LSW_{(u)}$ (red triangle, Figure 4.a). Previous work has shown that water at mid-depths in the Rockall Trough is composed of a layer of intermediate WTOW overlying a layer with properties approximating the *MOW*-*LSW* mixing line (e.g. Figure 2; Johnson *et al.*, 2010). As such it seems reasonable to assume mixing between water lying upon the two mixing lines rather than between individual water types. However, as a check we calculated the proportion of an artificial water type, *B*, defined as the intercept of mixing lines $UW_{(l)}$ -*NSDW* and *MOW*- $LSW_{(u)}$ (Figure 4.a). This gives an indication of the strength of the intermediate salinity inflexion (ISI, Figure 2) which marks the transition from the intermediate WTOW layer to the *MOW*-*LSW* mixture which enters the trough from the south. The maximum percentage of *B* exceeded 20 % for all but one of the cruises analysed suggesting that the intermediate salinity inflexion and therefore the intermediate WTOW and *MOW*-*LSW* layers were a persistent feature. The proportion of water type *NSDW* at any point in mixing triangle $UW_{(l)}$ - B - $LSW_{(u)}$ was calculated by multiplying the proportion of WTOW by the proportion of pseudo water type *B* and the proportion of *NSDW* at a point infinitesimally above point *B* on mixing line $UW_{(l)}$ - B -(*NSDW*).

A similar approach was used to calculate the proportion of deep WTOW in the western trough. Deep WTOW has characteristics intermediate to water lying upon mixing line *MOW*-*LSW* and *UW*-*NSDW* (Figure 2; Johnson *et al.*, 2010). As such, a new mixing triangle was

drawn (blue, Figure 4.a) with mixing again assumed to occur between these two mixing lines rather than individual water types. Deep WTOW with a density greater than that of $LSW_{(u)}$, was assumed to have formed from mixing between LSW and WTOW (yellow, Figure 4.a), or between $LSW_{(l)}$, AABW and WTOW (green, Figure 4.a) if the density exceeded that of $LSW_{(l)}$. Again mixing was calculated between the two appropriate mixing lines. The proportion of pure NSDW within the triangle or quadrangle was calculated by multiplying the proportion of mixing line $UW_{(l)}$ -NSDW by the proportion of NSDW at the corresponding point on the WTOW mixing line. A more detailed description of the mixing model can be found in Johnson (2012). Water mass analysis was carried out on each hydrographic section, including every EEL occupation between 1975 and 2015 with good quality data. Outputs from the model were smoothed over a 100 m window using a moving average. The results of the water mass analysis are reported in terms of the pure water masses. For example, a value of 100 % pure WTOW represents water with properties lying on mixing line $UW_{(l)}$ -NSDW (Figure 4.a). Similarly, a 100 % NSDW value reflects water with properties identical to water type NSDW.

4.1.2. Validation of mixing model

As a check on the performance of the mixing model, predicted CFC-11 concentrations along the EEL were computed and compared to observations made in September 1997 during cruise D230. If assumptions made within the mixing model were valid, and all water masses were accounted for, predicted and observed concentrations should match well. Predicted CFC-11 concentrations ($CFC_{predicted}$) were calculated by multiplying the proportions of individual water types during cruise D230 as outputted from the model, by CFC-11 concentrations of the individual water types:

$$CFC_{predicted}^i = P_{AABW}^i * CFC_{AABW} + P_{LSW}^i * CFC_{LSW} + P_{MOW}^i * CFC_{MOW} + P_{NSDW}^i * CFC_{NSDW} + P_{UW}^i * CFC_{UW}$$

Water type CFC-11 concentrations were determined from cruises at the upstream boundary of the Rockall Trough (Table 3) with the exception of LSW which was taken at the EEL latitude due to documented large spatial variability within the basin (New and Smythe-Wright, 2001). CFC-11 data for D230 were downloaded from the CLIVAR and Carbon Hydrographic Data Office (<http://cchdo.ucsd.edu>). All data were reported relative to the SIO-93 scale.

Predicted and observed CFC-11 profiles showed a good agreement (Figure 5) indicating that the mixing model worked well and assumptions made were valid. In particular the shape of the profiles, absolute concentrations and rates of change between successive inflexion points were reproduced well. However, the comparison suggested that the depth of the upper boundary of intermediate WTOW, as indicated by decreasing CFC-11 concentrations, was over-estimated by around 100 m in the mixing model. Predicted concentrations were also around 0.2-0.5 pmol kg⁻¹ higher than those measured at the seabed. This suggests that the model slightly underestimated the proportion of LSW in the basin; however, this discrepancy was small and at a depth below which WTOW was observed. Hence, we believe that the model performed well and is suitable for investigating the proportion of WTOW and its constituent water mass NSDW within the Rockall Trough.

4.1.3. Estimation of errors

Two potential sources of error within the mixing model were considered: those related to temporal changes in the $UW_{(t)}$ definition, and those linked to the instrument precision. UW properties within the Rockall Trough are known to vary with the strength of the subpolar gyre and the relative importance of southern versus subpolar water masses within the basin (Holliday, 2003; Johnson *et al.*, 2013). Although this was partially accounted for by using a time-varying $UW_{(t)}$ definition in the model, transport lags may mean that the WTOW observed at the EEL was formed by mixing with UW with different properties. The mean annual changes in $UW_{(t)}$ definitions were ± 0.01 for salinity and ± 0.16 °C. To allow for a lag of up to two years, water mass analysis was carried out using the original $UW_{(t)}$ definition, and an $UW_{(t)}$ definition plus twice the annual mean changes. The difference between the two cases was < 1 % for both the proportion of WTOW and NSDW at any point in the water column. However, the upper boundary of the WTOW layer did shift in the water column by around 100 m. Thus, whilst the water mass proportions were essentially unaffected, there was some error associated with the precise depth of the upper boundary of the intermediate WTOW layer.

The second source of error investigated was that resulting from the instrument noise associated with the conductivity sensor. The intra-cruise salinity variability was estimated by subtracting a smoothed profile (100 m moving average) from individual data points. To ensure that any differences were likely to be related to instrumental rather than oceanic variability, only the intermediate water column (σ_{θ} 27.45-27.65 kg m⁻³) in the eastern Rockall

Trough was examined; this area is known to have a tight θ - S relationship (Johnson *et al.*, 2010). A single estimate of variability for each cruise was calculated by taking a standard deviation of all absolute residuals within the defined density range. The water mass mixing model was then run twice: with the original data, and again with the instrumental variability added to the salinity values. The difference in the water mass proportions between these two cases gives an estimate of the error related to the instrumental precision. As expected, the largest errors were associated with water mass proportions determined from data collected in the 1970s and 1980s, and the smallest with data post 1992 after the introduction of the Neil Brown MK3 and Sea-Bird 911+ systems on the EEL. The mean error associated with the proportion of WTOW at any point in the water column for these two time periods were $\pm 10\%$ and $\pm 5\%$ respectively, whilst the mean errors associated with the proportion of NSDW were $\pm 4\%$ and $\pm 2\%$. Errors for the sections in the northern Rockall Trough (BRS, Figure 1) and between the northern banks (LG, Figure 1) were similar to the post-1992 EEL values.

4.2. Calculation of modified WTOW transport

4.2.1. Using OSNAP mooring array

The transport of WTOW in the central Rockall Trough was calculated using the first year of data from the OSNAP moorings. This flux estimate focusses on the deep component of WTOW ($> 27.65 \text{ kg m}^{-3}$) and therefore refers to the overflow water found below the intermediate salinity inflexion in the western trough only. We divided the water column around moorings WB1 and WB2 into six boxes with the microCAT CTD measurement points at their centre (Figure 3.b, Table 4). The upper limit of these boxes was the mean depth of the 27.65 kg m^{-3} isopycnal (1150 m) and the eastern extent the mid-point between the location of WB1 and station G on the EEL (-12.091°W). The lower and western bounds were the seabed. If a box did not have a current record at its centre (either due to mooring design or instrument failure, e.g. boxes *a*, *b*, *d* and *e*), one was constructed by linear interpolation of the records above and below it on the same mooring. As mean V velocities vary little with depth within the overflow layer at both WB1 and WB2 (Table 4), this step seems reasonable.

A transport time-series for each box was calculated by multiplying the area of the box by the V velocities. As a signature of deep WTOW is not always present at the EEL (Johnson *et al.*, 2010), this transport was subsequently weighted by the proportion of overflow water. A time-

series of the proportion of WTOW in each box was calculated using a simplified version of the water mass analysis detailed in section 4.1. As deep WTOW is a mixture between water lying on the MOW-LSW and WTOW mixing lines (Section 2; Johnson *et al.*, 2010), we first defined these (Figure 4.c). A mean eastern θ - S profile, approximating the MOW-LSW mixing line, was created by combining CTD data from the 2014 and 2015 EEL cruises (stations east of the Anton Dohrn Seamount only) with microCAT CTD data from mooring EB1 by averaging along isopycnals. Little spatial or temporal variability was observed about the mean. The WTOW mixing line was defined as in the full water mass mixing model, i.e. from the point at which the water properties move away from the Harvey (1982) ENAW mixing line, to NSDW (Table 2). For each time-step, i , within a microCAT record, two end members of a new mixing line (E_i - W_i , Figure 4.c) were then described. The first, E_i , being the point on the mean eastern profile with a potential density identical to that of the microCAT data point at time-step i ; and the second, W_i , the point on the WTOW mixing line with the same potential density. The proportion of pure WTOW at the microCAT data point (M_i) could then be calculated. If the volume transport was weighted by this value, it would give the transport of unmodified WTOW at the EEL latitude, i.e. the weighting would only be one if M_i lay on mixing line $UW(l)$ -NSDW. Unmodified WTOW is only observed close to the Wyville Thomson Ridge; by the time WTOW has reached the central Rockall Trough its properties have been modified by mixing with surrounding water masses (e.g. Figure 2; Johnson *et al.*, 2010). As such, a transport at the EEL latitude weighted by the proportion of pure WTOW would be an underestimate. In order to give a more realistic flux estimation, we therefore calculated the transport of modified WTOW. We defined this as any water containing greater than 50 % pure WTOW and thus calculated the proportion of modified WTOW by multiplying the proportion of pure WTOW by two with the maximum percentage being limited to 100 %. Indeed, in water mass analysis, the 50 % contour is sometimes used to define the boundary of a water mass (e.g. Mamayev, 1975; Silva *et al.*, 2009). The flux of modified WTOW at the EEL is around twice that of the flux of pure WTOW. Only one box (d) did not have a microCAT record. A time-series of the proportion of WTOW for this box was constructed using the relationships between records from surrounding boxes. The total WTOW transport on 12 hourly time-steps was calculated by summing the weighted transports for every box.

4.2.2. Using geostrophic method

In order to place the OSNAP transports in context, WTOW fluxes were also estimated using geostrophic velocities derived from all EEL occupations with good quality data. Geopotential anomalies at each pair of CTD stations were converted to geostrophic velocities using the CSIRO SEAWATER routines (v1.2d). To calculate absolute geostrophic velocities and transports, an assumption about a level of no/known motion must be made. Previous geostrophic calculations within the Rockall Trough have used a mid-depth level of no motion (Ellett and Martin, 1973; Holliday *et al.*, 2000; Holliday *et al.*, 2015). A comparison between geostrophic-derived and satellite-derived velocities, as well as the net transport balance within the basin, suggests that the assumption of zero flow at 1200 m is reasonable (Holliday *et al.*, 2000; Holliday *et al.*, 2015). Additionally, analysis of historical moorings at stations F and M on the EEL (Figure 3 for location) show a flow reversal at around this depth (Holliday *et al.*, 2000). However, new data from the OSNAP moorings suggest that this is not the case at both the eastern and western boundaries of the basin: mean V velocities are southwards throughout the water column at WB1 (range -7.7 to -10.7 cm s^{-1}), whilst only northward mean V values are observed at ADCP1 (range 10.2 to 15.3 cm s^{-1}). As such, we constructed a zonally varying reference velocity based on the mean mooring velocities. For the majority of the trough the geostrophic velocity at 1200 m was set to zero. However, at the western boundary geostrophic velocities were referenced to the mean V at 1360 m on WB1 (-10.7 cm s^{-1}). Similarly, the velocity at the seabed at the eastern boundary was referenced to the deepest mean V measured at ADCP1 (10.2 cm s^{-1}). Instead of referencing stations shallower than 1200 m (e.g. over the Anton Dohrn Seamount) to zero at the seabed, we set the deepest velocity to the measured mean V from a similar depth on the nearest mooring. Being shallow, these stations will only make a small or zero contribution to the WTOW flux calculations. Volume transports were again weighted by the proportion of WTOW at that point in the water column as determined by water mass analysis (section 4.1). As detailed in section 4.2.1, we calculated the transport of modified WTOW (i.e. that containing at least 50 % pure WTOW) rather than of pure WTOW. The total modified WTOW flux for each cruise was calculated by summing the weighted transports for water denser than 27.65 kg m^{-3} over the western trough. Transports within the bottom triangles (water below the deepest common depth level of each pair of CTD stations) were calculated by assuming both a constant velocity and proportion of WTOW equal to that at the deepest common level. These bottom triangle transports were added to the total WTOW transport and on average comprised < 10 % of the total modified WTOW flux.

5. Results of water mass analysis

5.1. *Overflow water in the northern Rockall Trough*

The results from water mass analysis on a section in the northern Rockall Trough (BRS, Figure 1), showed that WTOW is an important component of the water column (Figure 6.a). In the southern portion of the section, between Rosemary Bank and the Scottish Shelf, water comprised of > 50 % pure WTOW (grey, Figure 6.a) formed a 350-500 m thick layer situated below the UW and above the MOW-LSW layer. North of Rosemary Bank, however, the overflow layer was thicker (450-900 m) and extended to the seabed at a number of stations. As expected, the proportion of NSDW showed a similar distribution (Figure 6.b). In the southern half of the section values of 5-10 % were observed at intermediate depths, whilst to the north of Rosemary Bank proportions of > 15 % were observed at some locations. Two maximums in the NSDW distribution were seen: one at around 60 °N on the flank of Bill Baileys Bank, and a second at a similar depth but to the north of Rosemary Bank. It is important to note that this does not mean that water with the characteristics of pure NSDW (i.e. 34.91, -1.0°C, Table 2) is observed in the Rockall Trough. This would only be true if the percentage of NSDW was 100 %. However, the greater the percentage of NSDW, the closer the water properties are to unmodified NSDW. The sloping isopycnals in the northern half of the section (Figure 6.c) indicated shear within the water column and suggested westward flow of the overflow water into the central Rockall Trough.

5.2. *Overflow water between northern banks*

In order to investigate the possibility of flow from the Rockall Trough into the Iceland Basin through the channels between the northern banks, we now look at a section between George Bligh Bank and Lousy Bank (LG, Figure 1). The water column was composed nearly entirely of UW and WTOW, with only a very thin layer (~50 m thick) of the MOW-LSW mixture in the south of the channel (Figure 7.a). NSDW made up 15-20 % of the water column at the deepest levels, which was similar to that observed in the northern Rockall Trough despite the different timings of the surveys. The layer containing > 50 % pure WTOW (grey, Figure 7.a) was thicker near both Lousy Bank and George Bligh Bank, extending an additional 200 m and 50-100 m higher in the water column respectively in these locations. A similar doming

was observed in the 27.4 kg m^{-3} isopycnal (Figure 7.b) suggesting that there may have been a cyclonic recirculation within the channel. However, the 27.5 and 27.6 kg m^{-3} isopycnals were only sloped in the vicinity of Lousy Bank. This suggests that whilst the denser component of WTOW flowed north-westward in the north of the channel, there was no return flow in the south. Hence, the net transport of WTOW may have been from the Rockall Trough to the Iceland Basin.

5.3 Overflow water in the central Rockall Trough

Moving southwards to the central Rockall Trough (EEL, Figure 1), we first look at a single occupation from 2006 which had two extra stations in the western trough in addition to the standard EEL stations (Figure 8). Around 15 % of EEL cruises had a maximum NSDW proportion within the deep WTOW equivalent to, or greater than, the 2006 section. Thus the 2006 section represents a strong signature of deep WTOW but is not anomalous. Again, the difference between the eastern and western portions of the basin is clear. At intermediate depths (700-1100 m) water containing > 50 % pure WTOW formed a layer extending across the entire width of the trough (grey, Figure 8.a). However, in addition, a core of water composed of > 50 % pure WTOW was seen hugging the eastern flank of Rockall Bank between 1200 m and 1500 m. It is worth noting that the highest percentages within this deep core were observed at an additional station between standard EEL stations D and E. The deep component of WTOW can be more clearly identified by highlighting the 20 % or 40 % contour, and by looking at the NSDW percentages (Figure 8.b). Two cores of dense overflow water were seen: one situated between 1100-1700 m on the eastern flank of Rockall Bank, and the other at ~1750 m slightly further east at 11.8°W . The first core was associated with NSDW proportions of 20-25 %, whilst the secondary core was composed of 15-20 % NSDW. Again the sloping isopycnals in the vicinity of Rockall Bank (Figure 8.c) indicated strong shear and therefore baroclinic flow in this region.

The EEL time-series allows us to look at the persistence of the WTOW signature over the past 40 years. In order to fully resolve the deep component of the overflow, we focus on the proportion of NSDW in the water column. Despite the time-varying nature of WTOW, a clear signature of both intermediate and deep WTOW was seen with a core of overflow water hugging the eastern flank of Rockall Bank (Figure 9.a). However, the NSDW percentages within the deep component of the overflow are muted relative to the high values observed

during the 2006 cruise. Additionally, no secondary core near 11.8 °W was seen although the 2.5 % contour extended to east of this point and there was high variability in this region (Figure 9.b). Water column inventories (Figure 9.c), were calculated by multiplying the proportion of NSDW at each particular depth, by the depth of the bin associated with that data point. Values were then summed from the sea surface to sea bed. Again, a clear difference is seen between the eastern and western trough. The mean inventories at the four deep stations east of the Anton Dohrn Seamount were almost identical (mean \pm standard error, 25 ± 2 m) with only a slight decrease in the easternmost station due to its shallower depth. This NSDW inventory is attributable to the intermediate component of WTOW. Water column inventories in the western trough were higher with a clear west-east trend. The largest mean inventory (49 ± 4 m) was seen at the first westernmost station with a depth exceeding 1200 m (i.e. deep enough to see any influence of deep WTOW); with the smallest inventory observed at the easternmost station west of the seamount. It should be noted that the lowest mean water column inventory for the western trough (38 ± 5 m) was higher than any seen in the east of the basin. This additional inventory in the western trough can be attributed to the signal of deep WTOW (not shown); it ranges from 13 to 24 m with the greatest influence observed in the far west of the basin.

6. Transport estimates of modified WTOW

6.1. Mooring transports

Having established the clear presence of WTOW in the water column, we now present transport estimates calculated from the OSNAP mooring array. We focus on the deep component of WTOW; thus this flux is for water denser than 27.65 kg m^{-3} and describes the transport of WTOW below ~ 1200 m on the eastern flank of Rockall Bank. As mentioned in section 4.2, this flux is for WTOW modified by mixing rather than pure WTOW. During 2014-2015 nearly the entire WTOW flux (93 %) was observed by instruments on WB1 due to the higher V velocities and proportion of WTOW at this mooring (Table 4). V velocities at WB1 were an order of magnitude greater than those observed at WB2 (mean -9.4 cm s^{-1} and -0.9 cm s^{-1} respectively) suggesting that there was a strong zonal gradient of V velocities within the dense overflow. Similarly, the observed proportions of modified WTOW at WB1 (28-44 %) were greater than those at WB2 (2-20 %). Whilst the highest WTOW proportions

at WB1 were associated with the deepest measurement points on the mooring, this was not the case for WB2. Here, the largest proportion of WTOW was observed by the instrument located at 1595 m, around 200 m above the sea floor. Hence, at this longitude the core of the overflow water was slightly decoupled from the seabed.

The total flux throughout the near one year record was predominantly southward (Figure 10.a) with a mean transport and associated standard error of -0.3 ± 0.04 Sv (integral time-scale: ~ 7 days, degrees of freedom: 54). However, the flux was highly variable (standard deviation 0.3 Sv, range -1.2 to 0.6 Sv) with northward transports observed 15 % of the time. Whilst these were mainly for short periods lasting between 12 hours and a week (mean 2 days), a sustained stretch of positive V velocities was seen in January 2015 lasting 19 days. At the start of this period relatively high proportions of WTOW were still observed in the water column although this declined as the northward velocities persisted. For the record as a whole, a statistically significant positive correlation existed between the proportion of WTOW in the water column and the magnitude of the V velocities. However, the weak nature of this relationship (r 0.3, $p < 0.05$) suggested that there was not a simple association of increased southward transports related to a larger influence of overflow water.

6.2. Geostrophic transports

We now present transport estimates for the last 40 years calculated using the geostrophic method. Again the fluxes represent the transport of modified rather than pure WTOW and only account for the deep component of the overflow found below 27.65 kg m^{-3} on the eastern flank of Rockall Bank. A comparison between geostrophic-derived transports from the 2014 and 2015 EEL sections and values calculated from the OSNAP mooring array showed a fairly good agreement (Figure 10.a). Over the 40 years of EEL data, there was no long term trend in the WTOW transports with a mean and associated standard error of -0.3 ± 0.04 Sv (Figure 10.b). This was near identical to the 2014-2015 mean derived from the OSNAP array. However, the variability within the geostrophic transports was lower (standard deviation 0.3 Sv, range 1.0 Sv) than those observed in the OSNAP array (standard deviation 0.3 Sv, range 1.8 Sv). This may in part be related to the Summer bias of the EEL cruises (Holliday and Cunningham, 2013); slightly higher variability was observed at the OSNAP array during the Winter (November to April, standard deviation 0.3 Sv, range 1.8 Sv) than the Summer (May to October, standard deviation 0.2 Sv, range 1.4 Sv) although the difference is

small. Whilst the 1975 to 2015 mean geostrophic flux was southwards, northward transports were seen during 12 % of the record.

7. Discussion and conclusion

This paper has consolidated and extended the work of Johnson *et al.* (2010) in investigating the presence and distribution of WTOW in the Rockall Trough. This paper focusses on the deep component of WTOW with a density $> 27.65 \text{ kg m}^{-3}$. A clear signature of deep WTOW was observed in the northern Rockall Trough with isopycnals suggesting westward flow of the water mass at this location. In the central Rockall Trough, transports derived from geostrophy and the recently deployed OSNAP mooring array both reveal a mean southward flow. The propensity of density currents to keep bathymetry on their right in the Northern Hemisphere suggests that a flow pathway from the Wyville Thomson Ridge around the northern and western boundaries of the Rockall Trough is highly likely. Three moorings were deployed around the margins of the basin in 1978 (Figure 1, Table 1). By combining these records with those from the contemporary OSNAP moorings WB1 and WB2, we have a series of observations stretching from the Wyville Thomson Ridge around the boundary of the trough to the EEL. Although these two measurement campaigns are nearly 40 years apart, geostrophic transports show that the flow of WTOW through the basin is a persistent feature with no long term trend over this period (Figure 10). As such, with the lack of synoptic measurements, it seems reasonable to combine the information from these datasets. Mean current directions suggest that a flow pathway for the deep component of WTOW does indeed exist around the northern and western boundaries of the Rockall Trough (Figure 11). Mean speeds within this layer of deep WTOW are relatively high (mean $14 \pm 3 \text{ cm s}^{-1}$) with the largest value (27.9 cm s^{-1}) measured at the mooring closest to the Wyville Thomson Ridge (Table 1). A current meter record from the southern flank of Lousy Bank suggests possible westward flow of WTOW into the Iceland Basin at this location. A one-off hydrographic section across the channel between Lousy Bank and George Bligh Bank corroborates this finding. However, as transport fluxes at the Wyville Thomson Ridge and EEL are variable, the importance of this pathway is also likely to vary temporally.

Various studies within the Rockall Trough looking at sedimentary features indicative of strong bottom currents have been published. We compile these records (hatched areas, Figure

11) to show the spatial coherence of these features as well as the similarity to our results. Zones of erosion, which have been attributed to WTOW, have been observed on: the southern flanks of both Faroe Bank and Bill Baileys Bank (Boldreel *et al.*, 1998; Kuijpers *et al.*, 1998), the eastern slope of Lousy Bank (Due *et al.*, 2006) and the eastern margins of George Bligh Bank and Rockall Bank (Howe *et al.*, 2001). Westward flow in the channels between Bill Baileys Bank and Lousy Bank, and Lousy Bank and George Bligh Bank, has also been inferred (Due *et al.*, 2006; Kuijpers *et al.*, 1998). In contrast, no evidence of active erosion was seen in the channel between Faroe Bank and Bill Baileys Bank (Kuijpers *et al.*, 1998) which at < 600 m is too shallow for WTOW to enter it. Although the transport of WTOW within the Rockall Trough varies temporally, it is notable that these zones of erosion are seen over a depth range (800-2000 m) coincidental with that of deep WTOW as shown by our water mass analysis. This gives confidence that these features are related to the flow of deep WTOW around the boundary of the trough.

Water mass analysis using the 40-year EEL time-series reveals a persistent core of deep WTOW with a density > 27.65 kg m⁻³. The 1975-2015 mean proportion of NSDW within this deep WTOW is 5.0-7.5 % representing the time-varying nature of overflow water in the Rockall Trough. However, the maximum NSDW percentage within the water column exceeded 15 % in around a quarter of EEL cruises. Although percentages > 20 % NSDW were only observed 5 % of the time, we note that in 2006 the highest proportions were seen at an additional station intermediate to two standard EEL stations. Hence, an extra EEL station may be required to best capture the deep component of WTOW.

The mean flux of modified WTOW denser than 27.65 kg m⁻³ calculated using the OSNAP array is -0.3 ± 0.04 Sv (July 2014 to June 2015). A near identical long-term mean (-0.3 ± 0.04 Sv) was obtained from the 40 years of EEL data, although we note that the geostrophic velocities were referenced to the mean V velocities from long-term moorings, including those deployed as part of OSNAP. There is no trend in the geostrophic transports between 1975 and present. However, the transport of deep WTOW is highly variable with both the OSNAP record and 40 year EEL time-series showing northward transports 12-15 % of the time. Mean speeds within the deep WTOW layer on the western boundary of the Rockall Trough are around 10 - 15 cm s⁻¹ with a higher value measured by the mooring closest to the ridge (Table 1). This gives an estimated transport time for deep WTOW from the Wyville Thomson Ridge around the boundary of the trough to the EEL of less than 50 days. This is much less than the

18 month residence time estimated by Johnson *et al.* (2010) for the pool of less dense WTOW found in the intermediate water column, and represents the strong flow pathway for the deep component of the overflow around the boundaries of the basin. Thus we may expect to see fairly short-term variability in overflow at the ridge reflected in the OSNAP record. Transports at the Wyville Thomson Ridge show possible seasonality with increased fluxes in the Summer (Sherwin *et al.*, 2008; Sherwin and Turrell, 2005). Interestingly a strong seasonal signal is observed in the Faroe Bank Channel outflow with the highest transports again observed in the Summer (Hansen *et al.*, 2016). Although there is some evidence of reduced variability in the OSNAP record from May to October, the record is currently too short to comment robustly on any seasonal signal. Additionally, the EEL record is heavily biased towards the Summer months (Holliday and Cunningham, 2013). As more data becomes available from the OSNAP array we should be able to identify if there is any seasonality in WTOW transports in the Rockall Trough.

Water mass analysis on an EEL section from 2006 reveals the presence of a secondary overflow core slightly detached from the eastern flank of Rockall Bank ($\sim 11.8^\circ\text{W}$, Figure 8). Interestingly, results from the northern basin also show an offshore core ($\sim 59.6^\circ\text{N}$, Figure 6). We are unsure whether this feature results from a temporally varying secondary flow pathway slightly decoupled from the boundary of the basin, or from eddies which are thought to form as water overflows the Wyville Thomson Ridge (Stashchuk *et al.*, 2010). Indeed an eddy with WTOW as its core has been observed in the northern Rockall Trough (Ellett *et al.*, 1983). Regardless of its origin, the varying presence of this additional overflow core raises the possibility that the OSNAP moorings do not fully capture the entirety of the overflow and that the resultant transports may be an underestimate. The geostrophic calculations, which do include this location, however, show that transports associated with it are only a small component of the long-term mean flux ($\sim 5\%$). Hence we believe that the estimate of -0.3 ± 0.04 Sv of southward flow of modified WTOW at the EEL latitude is a reasonable one. As evidence suggests that some of the WTOW exits into the Iceland Basin via channels between the northern banks, we suggest that the volume transport may increase as one follows the flow pathway back around the boundaries of the trough to the Wyville Thomson Ridge. Unfortunately, modification of WTOW as it moves away from the ridge makes comparisons with previous transport estimates from this area (e.g. Sherwin *et al.*, 2008) difficult. As such we are currently unable to quantify how much overflow may enter

the Iceland Basin from the Rockall Trough. However, this pathway will be minor compared to that entering via the Faroe Bank Channel.

We hope that this work, along with that of Johnson *et al.* (2010), firmly places WTOW as a persistent water mass within the Rockall Trough. Whilst the flow pathways for intermediate WTOW remain somewhat uncertain (Johnson *et al.*, 2010), a clear pathway for deep WTOW is seen around the northern and western boundaries of the basin. We hope that this finding will aid future interpretations of both the EEL and OSNAP datasets.

Acknowledgements

This work was partly funded by NAACLIM, a project within the European Union 7th Framework Program (FP7 2007-2013) under grant agreement 308299. This work was also partly funded by NERC programme UK OSNAP (NE/K010875/1). During her PhD CJ received funding from: University of the Highlands and Islands, Funds for Women Graduates and the Thomas and Margaret Roddan Trust. The Extended Ellett Line programme is funded through UK NERC's National Capability programme. We thank the reviewers for their comments and time.

References

- Boldreel, L., Anderson, M., Kuijpers, A., 1998. Neogene seismic facies and deep-water gateways in the Faeroe Bank area, NE Atlantic. *Marine Geology* 152, 129-140 doi:10.1016/S0025-3227(98)00067-X.
- Bryden, H., Candela, J., Kinder, T., 1994. Exchange through the Strait of Gibraltar. *Progress in Oceanography* 33, 201-248 doi:10.1016/0079-6611(94)90028-0.
- Castro, C.G., Perez, F.F., Holley, S.E., Rios, A.F., 1998. Chemical characterisation and modelling of water masses in the Northeast Atlantic. *Progress in Oceanography* 41 (3), 249-279 doi:10.1016/S0079-6611(98)00021-4.
- Cuthbertson, A., Davies, P., Stashchuk, N., Vlasenko, V., 2014. Model studies of dense water overflows in the Faroese Channels. *Ocean Dynamics* 64, 273-292 doi:10.1007/s10236-013-0685-2.
- Dickson, R., Brown, J., 1994. The production of North Atlantic Deep Water, sources, rates and pathways. *Journal of Geophysical Research: Oceans* 99, 12319-12341 doi:10.1029/94JC00530.

- Due, L., van Aken, H., Boldreel, L., Kuijpers, A., 2006. Seismic and oceanographic evidence of present-day bottom-water dynamics in Lousy Bank-Hatton Bank area, NE Atlantic. *Deep Sea Research I* 53, 1729-1741 doi:10.1016/j.dsr.2006.08.006.
- Ellett, D., Kruseman, P., Prangmsma, G., Pollard, R., van Aken, H., Edwards, A., Dooley, H., Gould, W., 1983. Water masses and mesoscale circulation of north Rockall Trough waters during JASIN 1978. *Philosophical transactions of the Royal Society of London A* 308, 250-252 doi:10.1098/rsta.1983.0002.
- Ellett, D., Martin, K., 1973. The physical and chemical oceanography of the Rockall Channel. *Deep Sea Research and Oceanographic Abstracts* 20, 585-625 doi:10.1016/0011-7471(73)90030-2.
- Ellett, D., Roberts, D., 1973. The overflow of Norwegian Sea Deep Water across the Wyville-Thomson Ridge. *Deep Sea Research* 20, 819-835 doi:10.1016/0011-7471(73)90004-1.
- Fogelqvist, E., Blindheim, J., Tanhua, T., Østerhus, S., Buch, E., Rey, F., 2003. Greenland-Scotland overflow studied by hydro-chemical multivariate analysis. *Deep Sea Research I* 50, 73-102 doi:10.1016/S0967-0637(02)00131-0.
- Hansen, B., Larsen, K., Hátún, H., Østerhus, S., 2016. A stable Faroe Bank Channel overflow 1995-2015. *Ocean Science* (12), 1205-1220 doi:10.5194/os-12-1205-2016.
- Hansen, B., Østerhus, S., 2000. North Atlantic-Nordic Seas exchanges. *Progress in Oceanography* 45, 109-208 doi:10.1016/S0079-6611(99)00052-X.
- Harvey, J., 1982. θ -S relationships and water masses in the eastern North Atlantic. *Deep Sea Research* 29 (8), 1021-1033 doi:10.1016/0198-0149(82)90025-5.
- Harvey, J., Theodorou, A., 1986. The circulation of Norwegian Sea overflow water in the eastern North Atlantic. *Oceanologica Acta* 9, 393-402.
- Holliday, N., Cunningham, S., 2013. The Extended Ellett Line: Discoveries from 65 years of marine observations west of the UK. *Oceanography* 26, 156-163 doi:10.5670/oceanog.2013.17.
- Holliday, N.P., 2003. Air-sea interaction and circulation changes in the northeast Atlantic. *Journal of Geophysical Research: Oceans* 108, 2156-2202 doi:10.1029/2002JC001344.
- Holliday, N.P., Pollard, R., Read, J., Leach, H., 2000. Water mass properties and fluxes in the Rockall Trough, 1975-1998. *Deep Sea Research I* 47, 1303-1332 doi:10.1016/S0967-0637(99)00109-0.
- Holliday, N.P., S. Cunningham, C. Johnson, S. Gary, Griffiths, C., J. Read, Sherwin, T., 2015. Multidecadal variability of potential temperature, salinity, and transport in the eastern subpolar North Atlantic. *Journal of Geophysical Research: Oceans* 120, 5945-5967 doi:10.1002/2015JC010762.
- Howe, J., Stoker, M., Woolfe, K., 2001. Deep-marine seabed erosion and gravel lags in the northwestern Rockall Trough, North Atlantic Ocean. *Journal of the Geological Society, London* 158, 427-438 doi:10.1144/jgs.158.3.427.
- Humphreys, M., A. Griffiths, E. Achterberg, N. P. Holliday, V. Rerolle, J. Menzel Barraqueta, M. Couldrey, K. Oliver, S. Hartman, M. Esposito, Boyce, A., 2016. Multidecadal accumulation of anthropogenic and remineralised dissolved inorganic carbon along the Extended Ellett Line in the northeast Atlantic Ocean. *Global Biogeochemical Cycles* 30, 293-310 doi:10.1002/2015GB005246.
- Johnson, C., 2012. Tracing Wyville Thomson Ridge Overflow Water in the Rockall Trough, University of Aberdeen, available: <http://digitool.abdn.ac.uk>.
- Johnson, C., Inall, M., Häkkinen, S., 2013. Declining nutrient concentrations in the northeast Atlantic as a result of a weakening Subpolar Gyre. *Deep Sea Research I* 82, 95-107 doi:10.1016/j.dsr.2013.08.007.

- Johnson, C., Sherwin, T.J., Smythe-Wright, D., Shimmield, T., Turrell, W.R., 2010. Wyville Thomson Ridge Overflow Water: Spatial and temporal distribution in the Rockall Trough. *Deep Sea Research I* 57, 1153-1162 doi:10.1016/j.dsr.2010.07.006.
- Kirchner, K., Rhein, M., Mertens, C., Boning, C., Huttel, S., 2008. Observed and modeled meridional overturning circulation related flow into the Caribbean. *Journal of Geophysical Research Oceans* 113, 1-9 doi:10.1029/2007JC004320.
- Kuijpers, A., Anderson, M., Kenyon, N., Kunzendorf, H., van Weering, T., 1998. Quaternary sedimentation and Norwegian Sea overflow pathways around Bill Bailey Bank, northeastern Atlantic. *Marine Geology* 152, 101-127 doi:10.1016/S0025-3227(98)00066-8.
- Lee, A., Ellett, D., 1965. On the contribution of overflow water from the Norwegian Sea to the hydrographic structure of the North Atlantic Ocean. *Deep Sea Research and Oceanographic Abstracts* 12, 129-142 doi:10.1016/0011-7471(65)90019-7.
- Lozier, M., Stewart, N., 2008. On the temporally-varying northward penetration of Mediterranean Overflow Water and eastward penetration of Labrador Sea Water. *Journal of Physical Oceanography* 38, 2097-2103 doi:10.1175/2008JPO3908.1.
- Lozier, S., Bacon, S., Bower, A., Cunningham, S., de Jong, M., de Steur, L., de Young, B., Fischer, J., Gary, S., Greenan, B., Heimbach, P., Holliday, N., Houpert, L., Inall, M., Johns, W., Johnson, H., Karstensen, J., Li, F., Lin, X., Mackay, N., Marshall, D., Mercier, H., Myers, P., Pickart, R., Pillar, H., Straneo, F., Thierry, V., Weller, R., Williams, R., Wilson, C., Yang, J., Zhao, J., Zika, J., in press. Overturning in the Subpolar North Atlantic Program: a new international ocean observing system. *Bulletin of the American Meteorological Society* doi:10.1175/BAMS-D-16-0057.1.
- Mackas, D., Denman, K., Bennett, A., 1987. Least squares multiple tracer analysis of water mass composition. *Journal of Geophysical Research* 92, 2907-2918 doi:10.1029/JC092iC03p02907.
- Mamayev, O., 1975. *Temperature-salinity analysis of world ocean waters*. Elsevier Scientific Publishing Company.
- Mauritzen, C., Price, J., Sanford, T., Torres, D., 2005. Circulation and mixing in the Faroese Channels. *Deep Sea Research I* 52, 883-913 doi:10.1016/j.dsr.2004.11.018.
- Murray, S., Johns, W., 1997. Direct observations of seasonal exchange through the Bab el Mandab Strait. *Geophysical Research Letters* 24, 2667-2560 doi:10.1029/97GL02741.
- New, A., Smythe-Wright, D., 2001. Aspects of the circulation in the Rockall Trough. *Continental Shelf Research* 21, 777-810 doi:10.1016/S0278-4343(00)00113-8.
- Perez, F., Mintrop, L., Llinas, O., Glez-Davila, M., Castro, C., Alvarez, M., Kortzinger, A., Santana-Casiano, M., Rueda, M., Rios, A., 2001. Mixing analysis of nutrients, oxygen and inorganic carbon in the Canary Islands region. *Journal of Marine Systems* 28, 183-201 doi:10.1016/S0924-7963(01)00003-3.
- Rayner, D., Hirschi, J., Kanzow, T., Johns, W., Wright, P., Frajka-Williams, E., Bryden, H., Meinen, C., Baringer, M., Marotzke, J., Beal, L., Cunningham, S., 2011. Monitoring the Atlantic meridional overturning circulation. *Deep Sea Research II* 58, 1744-1753 doi:10.1016/j.dsr2.2010.10.056.
- Rhein, M., Kirchner, K., Mertens, C., Steinfeldt, R., Walter, M., Fleischmann-Wischnath, U., 2005. Transport of South Atlantic water through the passages south of Guadeloupe and across 16°N, 2000-2004. *Deep-Sea Research I* 52, 2234-2249 doi:10.1016/j.dsr.2005.08.003.
- Sherwin, T., Griffiths, C., Inall, M., Turrell, W., 2008. Quantifying the overflow across the Wyville Thomson Ridge into the Rockall Trough. *Deep Sea Research I* 55, 396-404 doi:10.1016/j.dsr.2007.12.006.
- Sherwin, T., Turrell, W., 2005. Mixing and advection of a cold water cascade over the Wyville Thomson Ridge. *Deep Sea Research I* 52, 1392-1413 doi:10.1016/j.dsr.2005.03.002.

- Silva, N., Rojas, N., Fedele, A., 2009. Water masses in the Humboldt Current System: Properties, distribution, and nitrate deficit as a chemical water mass tracer for Equatorial Subsurface Water off Chile. *Deep Sea Research II* 56, 1004-1020 doi:10.1016/j.dsr2.2008.12.013.
- Stashchuk, N., Vlasenko, V., Sherwin, T., 2010. Insights into the structure of the Wyville Thomson Ridge overflow current from a fine-scale numerical model. *Deep Sea Research I* 57, 1192-1205 doi:10.1016/j.dsr.2010.06.006.
- Stashchuk, N., Vlasenko, V., Sherwin, T., 2011. Numerical investigation of deep water circulation in the Faroese Channels. *Deep Sea Research I* 58, 787-799 doi:10.1016/j.dsr.2011.05.005.
- Tomczak, J., 1981a. A multi-parameter extension of temperature/salinity diagram for the analysis of non-isopycnal mixing. *Progress in Oceanography* 10, 147-171 doi:10.1016/0079-6611(81)90010-0.
- Tomczak, J.R., 1981b. An analysis in mixing in the frontal zone of South and North Atlantic Central Water off North-West Africa. *Progress in Oceanography* 10, 173-192 doi:10.1016/0079-6611(81)90011-2.
- Turrell, W.R., Slessor, G., Adams, R.D., Payne, R., Gillibrand, P.A., 1999. Decadal variability in the composition of Faroe Shetland Channel bottom water. *Deep Sea Research I* 46, 1-25 doi:10.1016/S0967-0637(98)00067-3.
- Ullgren, J., White, M., 2010. Water mass interaction at intermediate depths in the southern Rockall Trough, northeastern Atlantic. *Deep Sea Research I* 57, 248-257 doi:10.1016/j.dsr.2009.11.005.

Figure 1. Map of the northern and central Rockall Trough showing positions of hydrographic sections (red) and moorings (blue) used in this work. Circles denote historical mooring records obtained from the British Oceanographic Data Centre (www.bodc.ac.uk) and triangles contemporary records from the Rockall Trough portion of the OSNAP array. Also shown (black) are bathymetric features: AD: Anton Dohrn Seamount, BB: Bill Baileys Bank; FB: Faroe Bank; GB: George Bligh Bank; LB: Lousy Bank; RB: Rosemary Bank; RoB: Rockall Bank and W: Wyville Thomson Ridge.

Figure 2. Potential temperature-salinity diagrams from four locations in the Rockall Trough. Green: Knorr 147 (1996); light blue: Scotia 0804S (2004); red and blue: Discovery 312 (2006). Data for the southern Rockall Trough was obtained from WOCE (www.nodc.noaa.gov/woce), whilst other cruises data were obtained from the British Oceanographic Data Centre (www.bodc.ac.uk). ISI: Intermediate Salinity Inflexion; LSW: Labrador Sea Water; MOW: Mediterranean Overflow Water; NSDW: Norwegian Sea Deep Water; UW: Upper Waters. For interpretation see Section 2.

Figure 3. (a) Schematic of OSNAP moorings on the mean potential density field (kg m^{-3}) calculated from all EEL sections between 1996 and 2015; and (b) zoom-in of the western trough showing boxes used in the calculation of the modified WTOW flux from the OSNAP moorings. The 27.65 kg m^{-3} isopycnal, which was used as the upper bound of the deep WTOW in the flux calculations, is highlighted by the thick grey line. Instrument types are shown by the different symbols. Also shown (small black triangles) are the position of standard EEL stations. EEL stations in the Rockall Trough (west to east) are named B-Q, Q1 and R.

Figure 4. (a) Graphical representation of water mass mixing model and (b) detail of mixing triangle and percentage nomogram used to analyse intermediate waters. (c) Schematic of the simplified mixing model used in the calculation of modified WTOW transports from the OSNAP mooring array. Water types are shown by filled black circles (Table 2). Also shown in (a) and (b) is pseudo water type *B* and the intermediate salinity inflexion point (*ISI*). Small grey dots in (c) show data from the microcat at 1590 m on mooring WB1. The grey circle (M_i) in (c) is the MicroCAT temperature and salinity at an individual time-step *i*, whilst E_i and W_i are the two end-members for the mixing calculation.

Figure 5. Comparison of (a) observed and (b) predicted CFC-11 concentrations used to check assumptions made within the water mass mixing model. Predicted CFC-11 concentrations were calculated by multiplying output from the model for September 1997 by water type CFC-11 concentrations (Table 3, section 4.1.2). Observed CFC-11 values were collected at selected stations along the EEL in September 1997 (D230); data were downloaded from the CLIVAR and Carbon Hydrographic Data Office (<http://cchdo.ucsd.edu>). Only deep stations are shown. CFC-11 values are reported relative to the SIO-93 scale.

Figure 6. Results of water mass analysis across a section in the northern Rockall Trough occupied in May 2004 (BRS, Figure 1). (a) Percentage of pure WTOW with water containing greater than 50 % pure WTOW highlighted in grey. (b) Percentage of NSDW in the water column. (c) Contours of potential density (kg m^{-3}). A value of 100 % pure WTOW represents water with properties on mixing line $UW_{(l)}\text{-NSDW}$ (Figure 4.a). Similarly, a 100 % NSDW value reflects water with properties identical to water type *NSDW* (Figure 4.a). Small black triangles show location of CTD stations.

Figure 7. Results of water mass analysis across a section between two of the northern banks (Lousy Bank to George Bligh Bank) occupied in October 1996 (LG, Figure 1). (a) water containing greater than 50 % pure WTOW highlighted in grey with black contours showing percentage NSDW. (b) contours of potential density (kg m^{-3}). A value of 100 % pure WTOW represents water with properties on mixing line $UW_{(l)}\text{-NSDW}$ (Figure 4.a). Similarly, a 100 % NSDW value reflects water with properties identical to water type *NSDW* (Figure 4.a). Small black triangles show location of CTD stations.

Figure 8. Results of water mass analysis from a single occupation of the EEL section in the central Rockall Trough during October 2006 (EEL, Figure 1). (a) percentage of pure WTOW with water containing greater than 50 % pure WTOW shaded in grey. (b) percentage of NSDW in the water column. (c) contours of potential density (kg m^{-3}). A value of 100 % pure WTOW represents water with properties on mixing line $UW_{(l)}\text{-NSDW}$ (Figure 4.a). Similarly, a 100 % NSDW value reflects water with properties identical to water type *NSDW* (Figure 4.a). Small black triangles show location of standard EEL CTD stations whilst white triangles show two additional in-fill stations.

Figure 9. (a) Long-term mean percentage NSDW determined from water mass analysis carried out on all good quality EEL occupations between 1975 and 2015; and (b) the associated standard error. A value of 100 % NSDW reflects water with properties identical to water type *NSDW* (Figure 4.a). Small black triangles show location of standard EEL CTD stations and dashed line shows mean position of 27.65 kg m^{-3} isopycnal. (c) Long term mean water column inventories of NSDW at each EEL station deeper than 1000 m and associated standard errors. Water column inventories were calculated by multiplying the proportion of NSDW at each particular depth, by the depth of the bin associated with that data point. Values were then summed from the sea surface to sea bed.

Figure 10. Time-series of transports (S_v) of modified WTOW denser than 27.65 kg m^{-3} at the EEL latitude. (a) Flux calculated from OSNAP mooring array at 12 hour time-steps; and (b) Flux calculated from geostrophic velocities referenced to mean V velocities derived from moorings. Modified WTOW is defined as water which contains greater than 50 % pure WTOW. Grey circles in (a) show geostrophic derived fluxes for EEL cruises in July 2014 and June 2015. Methods used are described in section 4.2. Negative values indicate southward flow.

Figure 11. Compilation of evidence for flow pathways of deep WTOW in the northern and central Rockall Trough. Circles indicate location of moorings with associated arrows showing the mean flow direction within the deep WTOW core (Table 1). Black lines show position of hydrographic sections with arrows representing the flow direction within the deep WTOW as indicated by isopycnals (Figures 6-8). Hatched areas denote zones of bottom sediment erosion attributed to WTOW by several studies (Boldreel et al., 1998; Kuilipers et al., 1998; Howe et al., 2001; Due et al., 2006). Our θ - S analyses (e.g. Figures 6-8) confirm that WTOW is in contact with the seabed in these areas. Bathymetric features: BB: Bill Baileys Bank; FB: Faroe Bank; GB: George Bligh Bank; LB: Lousy Bank; RoB: Rockall Bank.

Table 1. Details of historical and contemporary moored current meter measurements in the deep WTOW layer around the northern and western boundaries of the Rockall Trough. All data were filtered to remove tides and inertial oscillations. Moorings I1, I2 and I3A were deployed in July 1978 with data obtained from BODC. Moorings WB1 and WB2 were deployed in July 2014 as part of the OSNAP project. Locations of moorings are shown in

Figure 1. Note that mooring WB2 is slightly removed from the boundary explaining the increased variability in flow direction.

Mooring id	Latitude (°N)	Longitude (°W)	Duration (days)	Sensor depth (m)	Direction (°) mean \pm std	Speed (cm s ⁻¹) mean \pm std
I2	60.195	9.257	54	972	202 \pm 49	29.7 \pm 15.9
I1	59.987	12.152	40	1066	304 \pm 95	10.6 \pm 7.6
I3A	58.930	13.252	255	1531	175 \pm 55	12.6 \pm 8.8
WB1	57.471	12.705	340	1585	179 \pm 79	15.5 \pm 9.8
WB2	57.470	12.331	340	1793	213 \pm 145	17.3 \pm 7.4

Table 2. Definitions of the water types influencing the Rockall Trough and used as end members in the water mass mixing model (Figure 4, section 4.1). The value for AABW was determined from previous analysis of EEL data (Holliday et al., 2000) whilst the values for MOW and NSDW were obtained from studies at the southern and northern boundaries of the Rockall Trough respectively (Hansen and Østerhus, 2000; Ullgren and White, 2010). The definitions for $UW_{(l)}$, $LSW_{(u)}$ and $LSW_{(l)}$ were determined individually for each cruise due to the temporally varying nature of these water masses (see section 4.1). A time-series of $UW_{(l)}$ definitions is similar to observed variations in upper water properties (Holliday et al., 2015), and in θ - S space the points lie on a mixing line between southern and subpolar water masses (as seen for upper waters in Johnson *et al.*, 2013). A time-series of $LSW_{(u)}$ definitions is again similar to variations in LSW properties within the Rockall Trough (Holliday et al., 2015).

Abbreviation	Full name	θ - S definition (reference)
AABW	Antarctic Bottom Water	34.95, 2.8 °C (Holliday et al., 2000)
$LSW_{(l)}$	Labrador Sea Water (lower bound)	point 0.005 below LSW salinity min.
$LSW_{(u)}$	Labrador Sea Water (upper bound)	point 0.005 above LSW salinity min.
MOW	Mediterranean Overflow Water	35.5, 9.0 °C (Ullgren and White, 2010)
NSDW	Norwegian Sea Deep Water	34.91, -1.0 °C (Hansen and Østerhus, 2000)

$UW_{(l)}$	Upper Water (lower bound)	departure in θ - S space from Harvey (1982) ENAW mixing line
------------	------------------------------	---

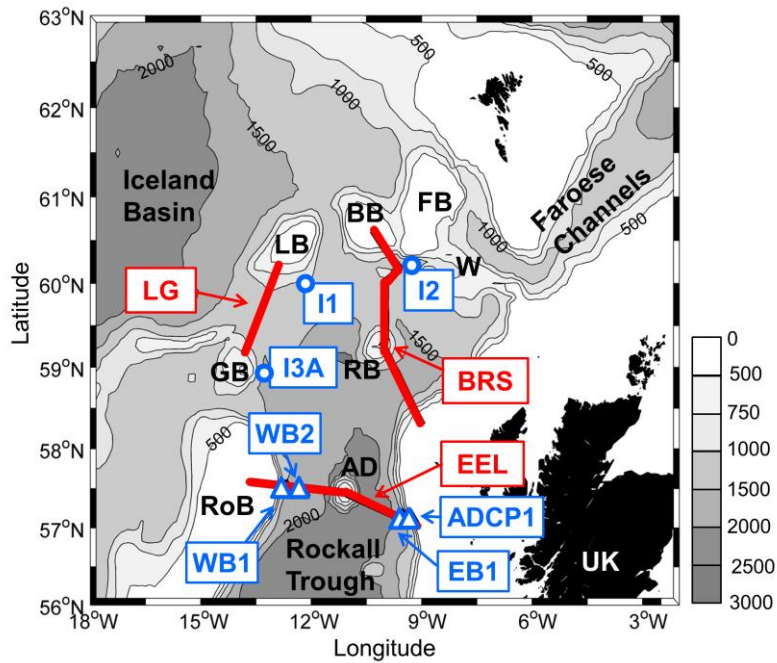
Table 3. Details of the water type CFC-11 concentrations used to check the assumptions made within the water mass mixing model (section 4.1.2). Source column details the cruise, year and location of the definition. Data from D230 and M39-5 were downloaded from the CLIVAR and Carbon Hydrographic Data Office (<http://cchdo.ucsd.edu>), whilst data from 34AR was downloaded from the International Council for the Exploration of the Sea (<http://ices.dk/ocean/project/veins>). All data are reported relative to the SIO-93 scale. Abbreviations: FSC: Faroe Shetland Channel; RT: Rockall Trough; WTR: Wyville Thomson Ridge.

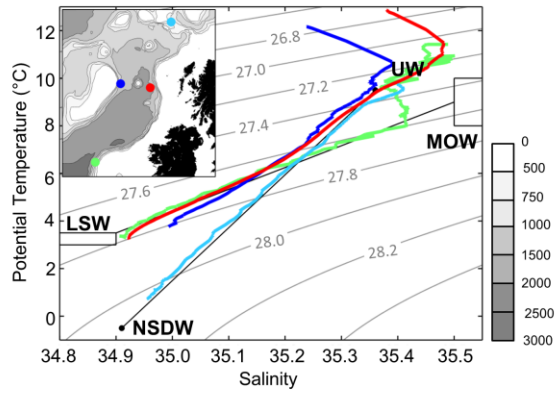
Water type	[CFC-11] (pmol kg^{-1})	Source (cruise, year, location)
<i>AABW</i>	0.5	D230, 1997, southern boundary RT
<i>LSW(l)</i>	2.0	D230, 1997, EEL
<i>LSW(u)</i>	2.0	D230, 1997, EEL
<i>MOW</i>	1.9	M39-5, 1997, southern boundary RT
<i>NSDW</i>	1.2	34AR, 1997, southern FSC
<i>UW(l)</i>	3.8	1994, Fogelqvist et al., 2003, WTR

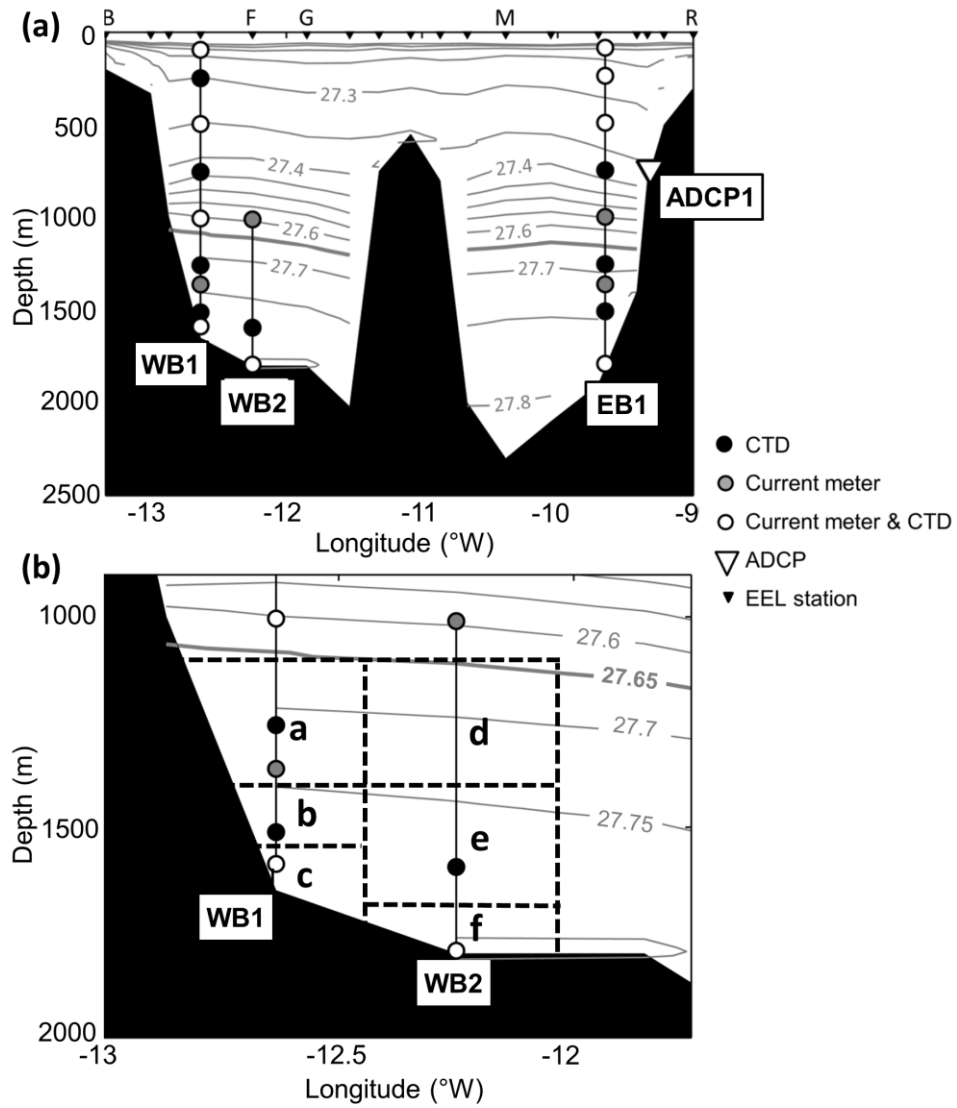
Table 4. Details of boxes used in the calculation of the transport of modified WTOW denser than 27.65 kg m^{-3} in the Rockall Trough using the OSNAP mooring array. $pWTOW$ denotes the proportion of modified WTOW whilst negative V velocities and transports indicate southward flow. The boxes are shown schematically on Figure 3.b. The eastern limit of boxes *a-c* is the mid-point between moorings WB1 and WB2, whilst the eastern extent of boxes *d-f* is the mid-point between mooring WB2 and EEL station G. The western bound of boxes *a-c* is the seabed. The upper limit of boxes *a* and *d* is the mean depth of the 27.65 kg m^{-3} isopycnal, and the lower extent of boxes *c* and *f* the seabed. The bounds between vertical boxes are calculated as the mid-depth between consecutive instruments.

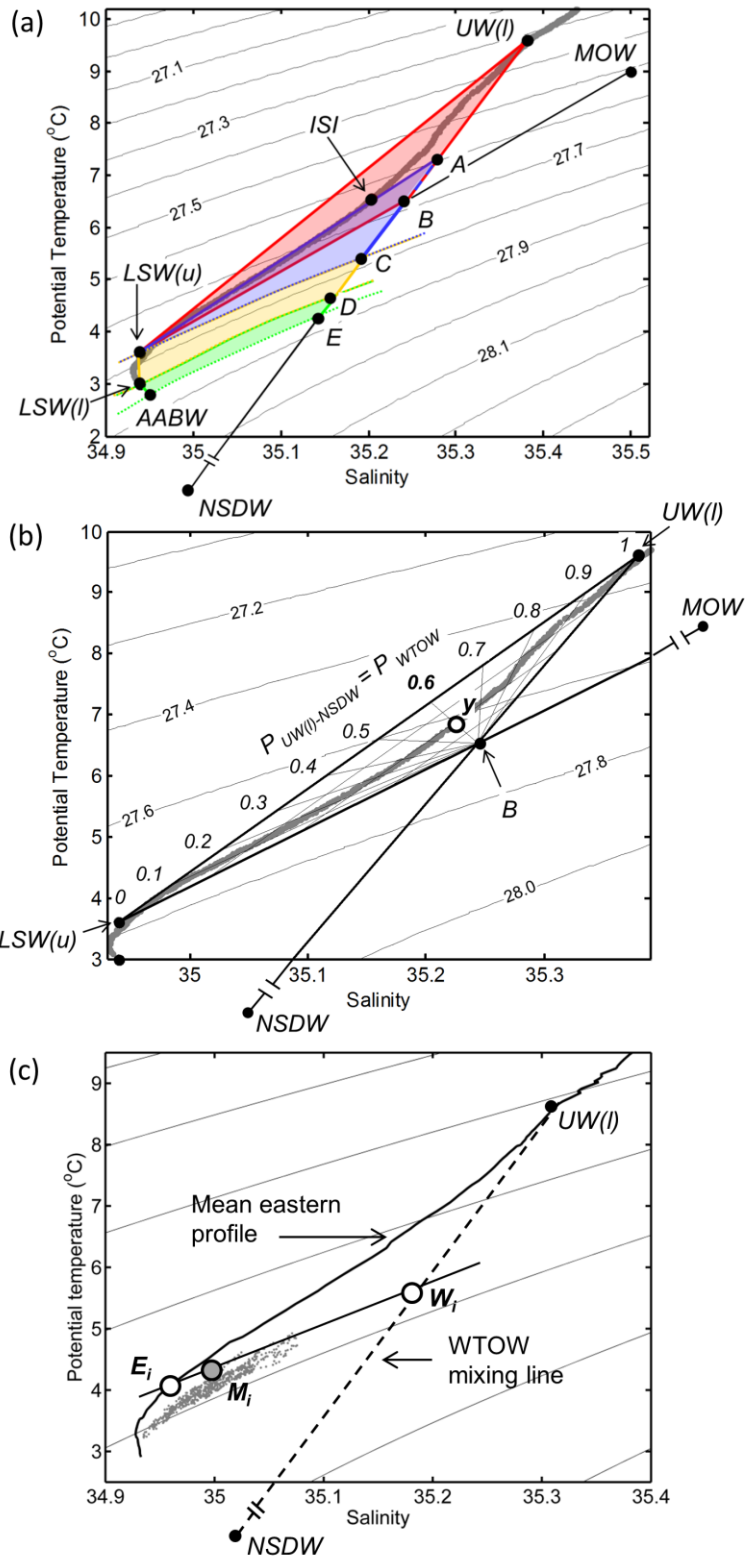
Box	Box centre	Area	V (cm s^{-1})	$pWTOW$ (%)	Transport (Sv)
-----	------------	------	----------------------------	-------------	---------------------------

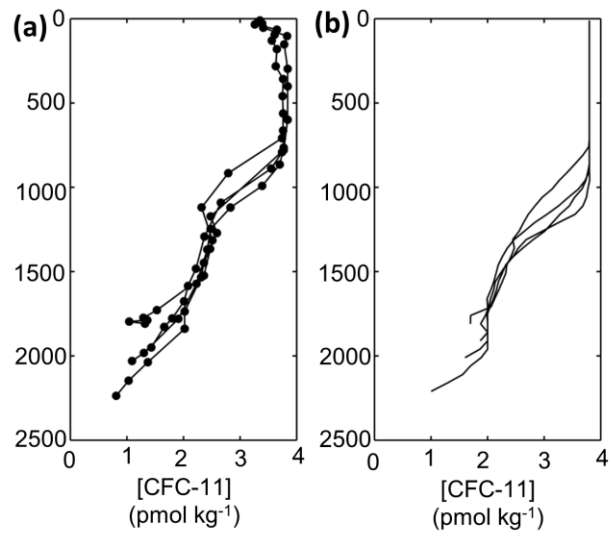
		($1 \times 10^6 \text{ m}^2$)	mean \pm std	mean \pm std	mean \pm std
<i>a</i>	WB1, 1255 m	3.5	-10.4 ± 8.4	28 ± 27	-0.11 ± 0.14
<i>b</i>	WB1, 1510 m	1.8	-9.3 ± 9.1	48 ± 25	-0.08 ± 0.08
<i>c</i>	WB1, 1590 m	1.1	-8.6 ± 9.9	44 ± 26	-0.04 ± 0.05
<i>d</i>	WB2, 1255 m	6.9	-0.5 ± 5.0	8 ± 6	0.00 ± 0.03
<i>e</i>	WB2, 1595 m	6.8	-1.0 ± 5.0	20 ± 19	-0.02 ± 0.11
<i>f</i>	WB2, 1795 m	2.3	-1.3 ± 5.5	2 ± 6	0.00 ± 0.01
Total					-0.25 ± 0.28

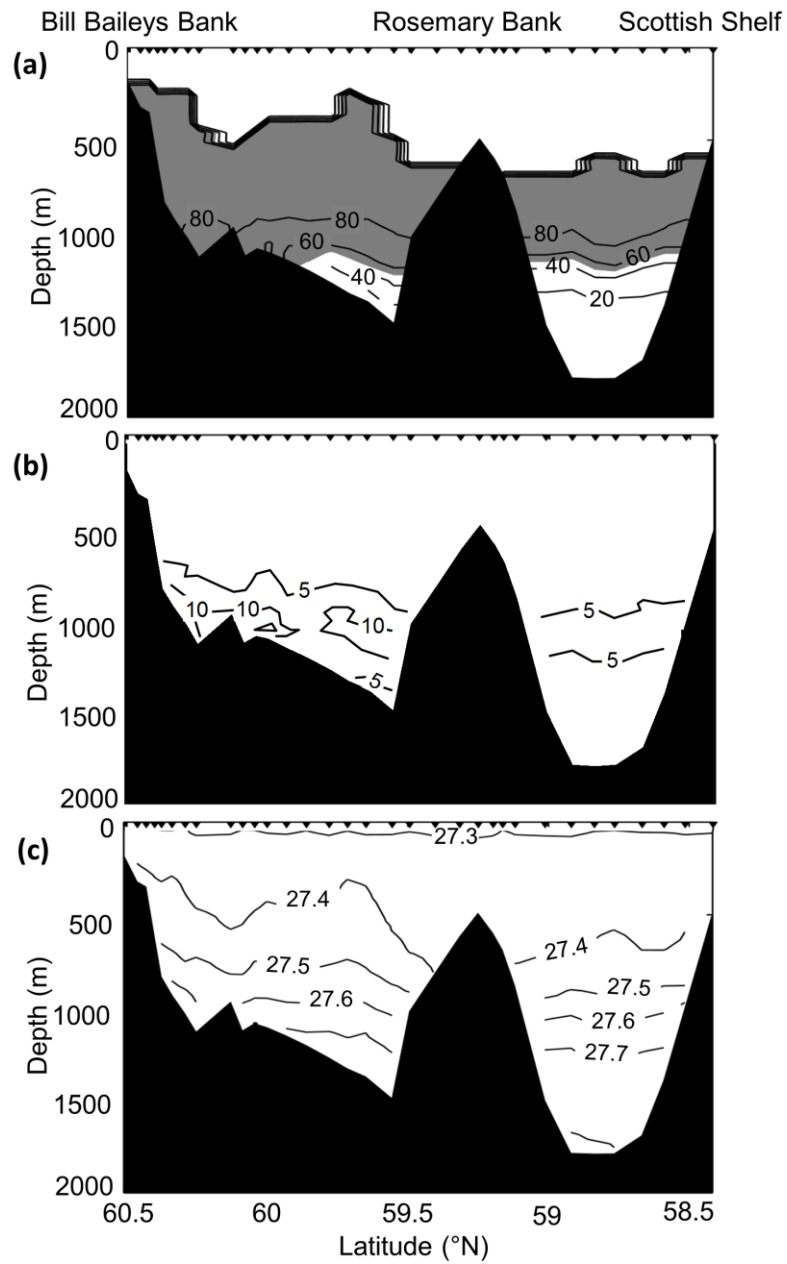


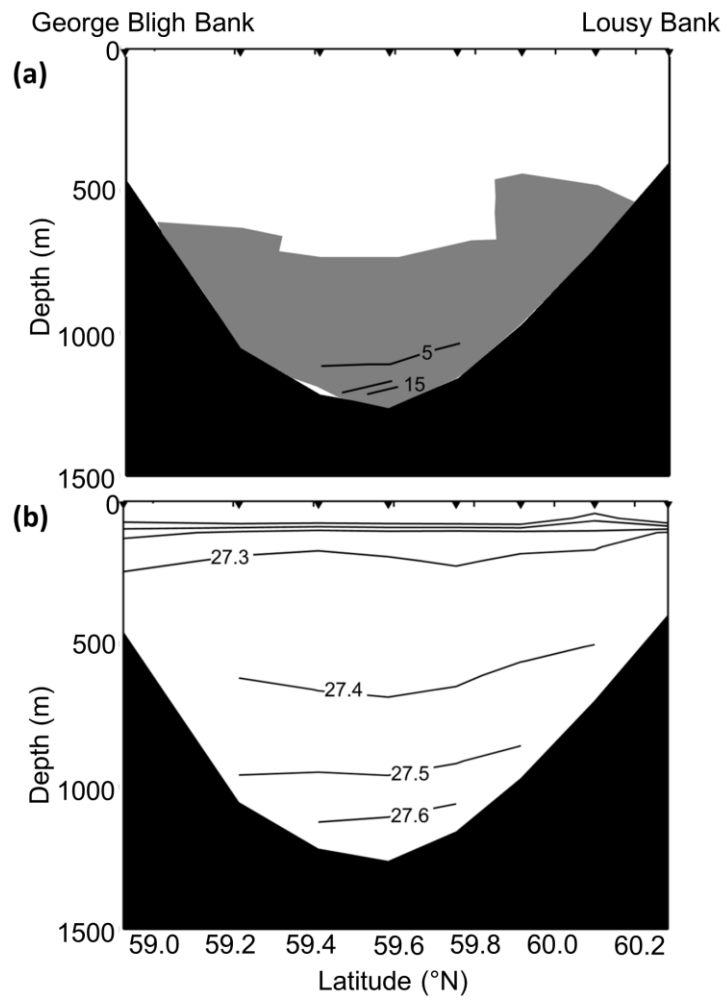


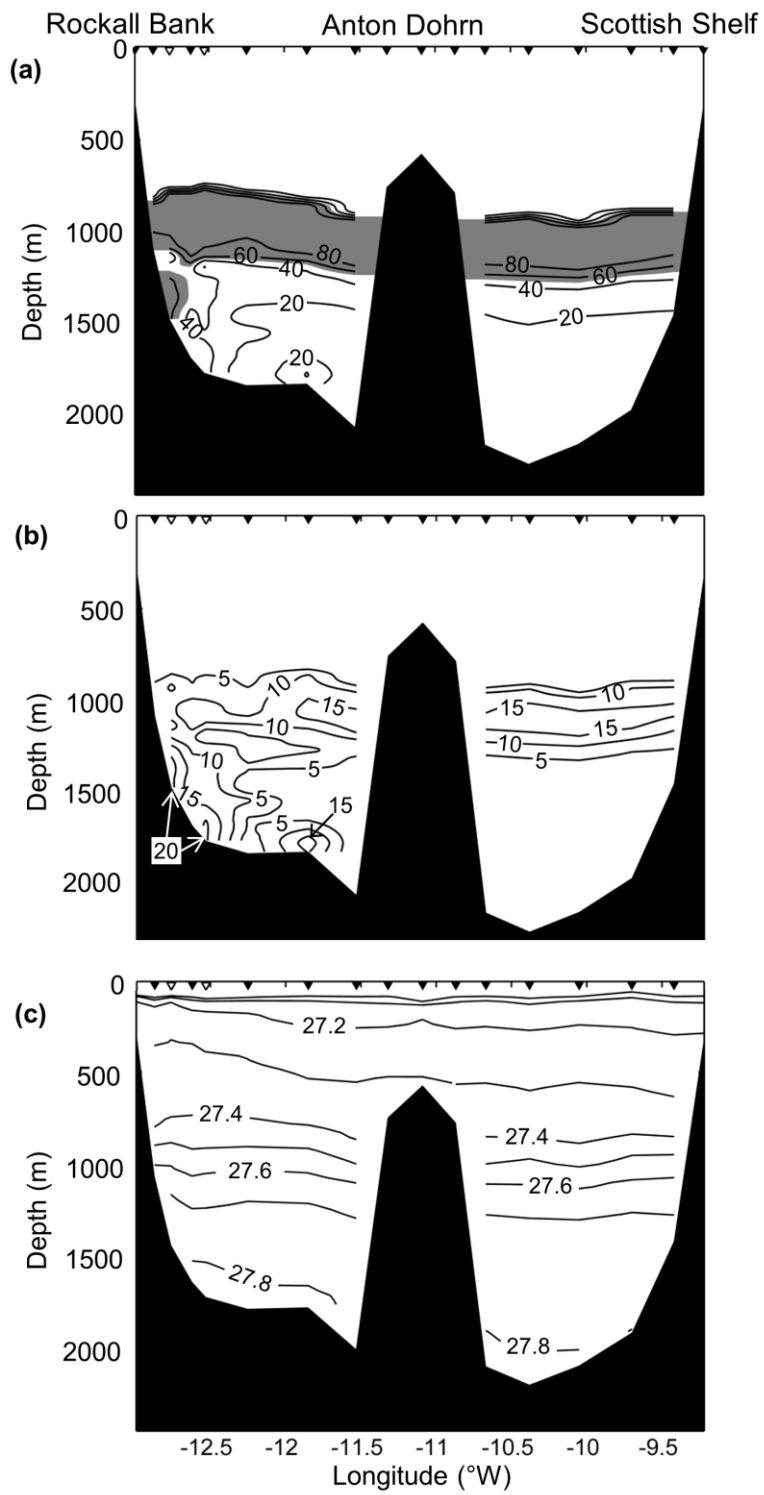


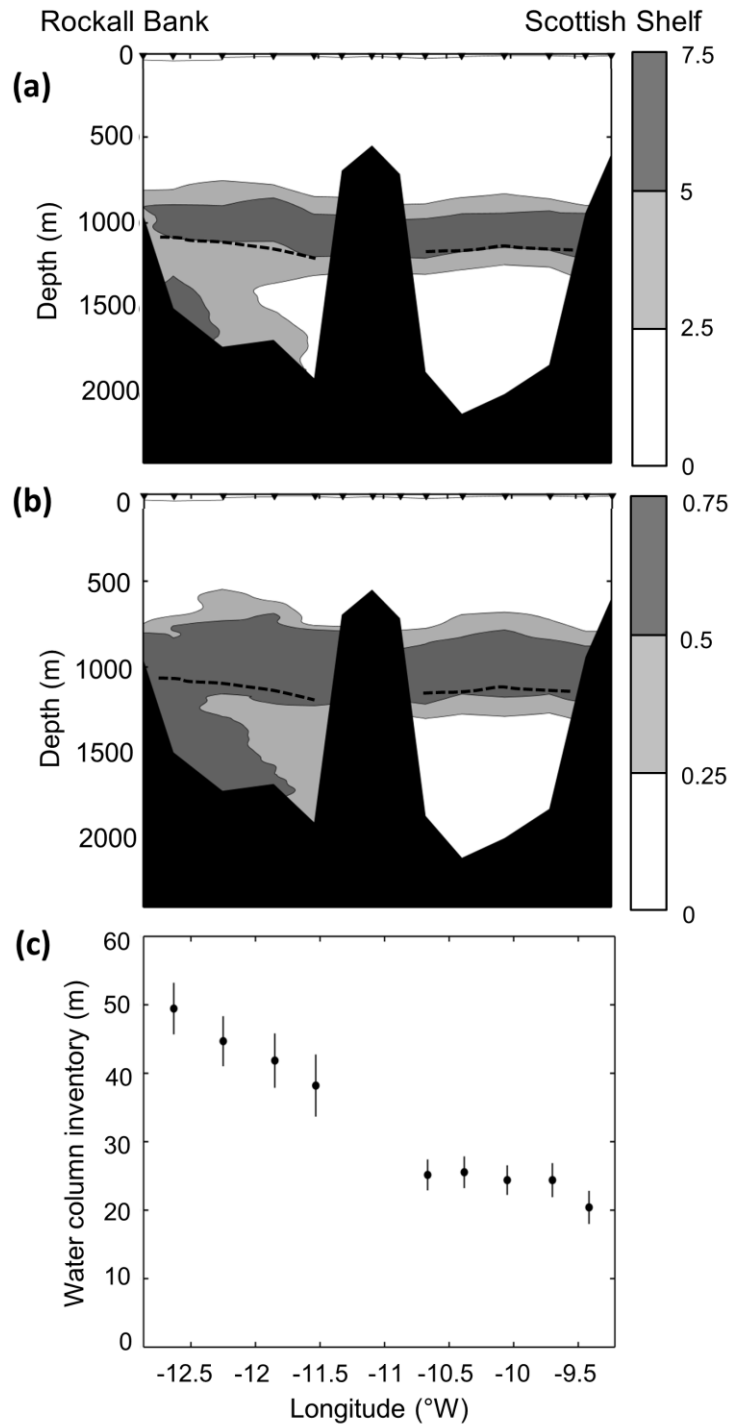


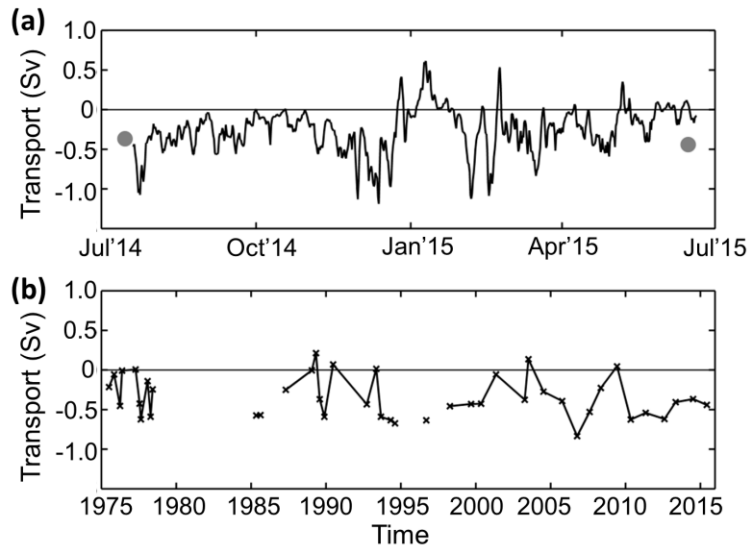


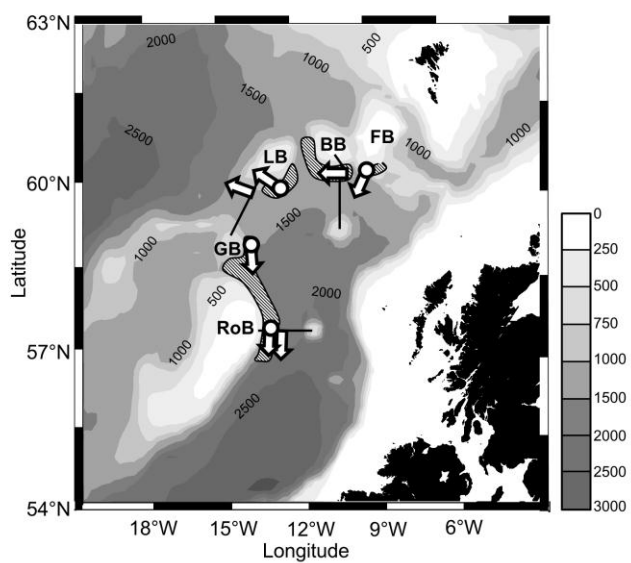












Accepted man